THREE-DIMENSIONAL SURFACE CURVATURE ESTIMATION USING QUADRIC SURFACE PATCHES

Ioannis Douros
Bernard Buxton

Department of Computer Science
University College London
Gower Street
London WC1E 6BT
United Kingdom

tel: ++44 (0) 20 7679 3695
fax: ++44 (0) 20 7387 1397

e-mail: {i.douros, b.buxton}@cs.ucl.ac.uk

Three-Dimensional Surface Curvature Estimation using Quadric Surface Patches

Recent advances in 3D scanning technology have enabled the development of interesting applications of 3D human body modelling and shape analysis, especially in the areas of virtual shopping, custom clothing and sizing surveys for the clothing industry. Most of the current applications have so far been concerned with automatic tape measurement extraction, i.e. simulation of the manual procedure for extracting a set of body measurements by conventional means, such as tapes and callipers. This has been an important advance since it has made it possible to extract in a non-intrusive manner sets of measurements in a few seconds rather than in the usual 40-45 minutes that also involve intrusive physical contact. However, this approach has a number of problems, and also fails to exploit the full potential of 3D imaging technology, as the 3D sets obtained by a scanner are still reduced to a collection of 1D measurements in order to describe body shape. The approach we present is a method for detecting significant geometric features on the 3D body surface. These features (such as ridges and umbilic points) require no a-priori anatomical information and can be used for driving matching and modelling algorithms such as deformable Active Shape Models. The approach is truly hardware-independent and will work on any set of reasonably complete 3D data, whether it is a raw point cloud or a pre-processed, canonical-type representation. Potential applications include sophisticated Shape Analysis techniques that may be used for classification of body types.

Estimation de Curvature des Surfaces 3D par Surfaces Quadriques

Les progrès récents de la technologie des scanners 3D ont permis le développement d'applications intéressantes sur la modélisation du corps humain et l'analyse de formes, en particulier dans le domaine de l'habillement, pour la vente virtuelle, l'habillement traditionnel (habit sur mesure), et des études sur les tailles. La plupart des applications actuelles se sont intéressées à l'extraction automatique de mesures, c'est-à-dire la simulation des procédures manuelles de mesures corporelles par des moyens conventionels, tel qu'un mètre de couturière ou un compas. Ceci a été une avancée significative puisque cela permet d'extraire d'une façon non-indiscrète un ensemble de mesures en quelques secondes au lieu des 40-45 minutes habituelles qui impliquent également un contact physique indiscret.. Cependant, cette approche comporte certains problèmes, et ne permet pas d'exploiter complètement le potentiel de la technologie d'imagerie 3D, puisque l'ensemble de données 3D obtenues par un scanner est toujours reduit à une collection de mesures 1D pour décrire la forme du corps. L'approche que nous présentons est une méthode pour détecter des aspects géométriques significatifs sur une surface 3D décrivant le corps humain. Ces aspects, tels des arêtes ou points umbiliques, ne nécessitent pas d'information préalable sur l'anatomie, et peuvent être utilisés par des algorithmes d'appareillement et de modélisation tels que les 'Active Shape Models' déformables. Cette approche est dépendante du matériel utilisé et marche sur tout ensemble de données 3D raisonnablement complètes, que ce soit un nuage de points grossiers ou une représentation de type canonique et pré-calculée. Les applications potentielles comprennent les techniques d'analyse de formes sophistiquées, qui peuvent être utilisées pour la classification de types de corps.

Three-Dimensional Surface Curvature Estimation using Quadric Surface Patches.

Ioannis Douros[✣], Bernard F. Buxton
Department of Computer Science
University College London

Abstract: Recent advances in 3D scanning technology have enabled the development of interesting applications of 3D human body modelling and shape analysis, especially in the areas of virtual shopping, custom clothing and sizing surveys for the clothing industry. Most of the current applications have so far been concerned with automatic tape measurement extraction, i.e. simulation of the manual procedure for extracting a set of body measurements by conventional means, such as tapes and callipers. This has been an important advance since it has made it possible to extract in a non-intrusive manner sets of measurements in a few seconds rather than in the usual 40-45 minutes that also involve intrusive physical contact. However, this approach has a number of problems, and also fails to exploit the full potential of 3D imaging technology, as the 3D sets obtained by a scanner are still reduced to a collection of 1D measurements in order to describe body shape. The approach we present is a method for detecting significant geometric features on the 3D body surface. These features (such as ridges and umbilic points) require no a-priori anatomical information and can be used for driving matching and modelling algorithms such as deformable Active Shape Models. The approach is truly hardware-independent and will work on any set of reasonably complete 3D data, whether it is a raw point cloud or a pre-processed, canonical-type representation. Potential applications include sophisticated Shape Analysis techniques that may be used for classification of body types.

Keywords: feature tracking, curvature estimation, matching, registration, 3D human body modelling.

1. Introduction

This work is concerned with the construction of curvature maps for 3D surface data acquired using Body scanning hardware. A further objective is to classify each point in the surface in a manner that allows the detection of geometric features as well as the initialisation of matching algorithms. Such algorithms are useful for a number of human body modelling applications, especially in the areas of clothing design and manufacturing (electronic tape measure, body shape analysis, garment sizing) and medical research (nutritional disorders, child growth, self perception, prosthetics design).

The subject of calculating curvature maps of 3D surfaces represented as digitised data (point clouds, range data, triangulated meshes) is not a new one. As illustrated in section 2, quite a lot of work has been done *around* the subject. This work differs from previous relevant research in that it takes into account the peculiarities of 3D body scanner data. There is currently a variety of 3D scanners available in the market with varying capabilities and features, but not yet a standard for representing data from any scanner. This poses a problem for algorithms and systems developers who wish to develop hardware-independent software, and often have to resort to the 'lowest-common-denominator' type of non-proprietary 3D scanner data representation. This is usually a dense and relatively noise-free point cloud, but may often contain significant gaps in the surface coverage. Moreover, it usually comes without any (useful) connectivity information, and almost always unaccompanied by any form of camera location information.

In the past 20 years, various researchers have developed a number of remarkable algorithms for calculating the curvature of digitised 2D curves and 3D surfaces. However, existing work is mainly focused:

- on voxel data, rather than on range data;
- on man-made (CAD) objects, rather than on free-form natural objects (such as human bodies);
- on pre-determined types of 2^{nd} degree patches (e.g. ellipse-specific), rather than for generic types;
- on 2D data rather than for 3D data;
- on 3D data with one dimension (say z) singled out, i.e. functions of the form $z = f(x,y)$ (Monge form).

The latter case is very frequently encountered, especially in the 3D surface curvature literature. Although it is sufficient for the theoretical study of the differential geometry of 3D surfaces, it is not really suitable for 3D point data acquired by using scanning hardware. This work bridges the gap by providing an algorithm that works for free-form 3D range data, with all three dimensions having equal importance and with no assumptions about the special cases of the geometric entity fitted (i.e. a generic quadric is fitted, that degenerates *automatically* into an ellipse, paraboloid or

✣ e-mail: i.douros@cs.ucl.ac.uk

hyperboloid according to the data). This can then be used to drive matching and registration algorithms, [Hilt99][Hutt01] or even PDM's for active shape models CTCG95].

2. Previous work

A detailed general overview of the concepts related to the differential geometry of 3D surfaces can be found in [Krey59]. The use of curvature information for analysing and studying surface shape is compiled in detail in the works of Porteous ([Port94] – focal surfaces, ridges, umbilics) and Giblin ([BrGT96] - ridges, crests, subparabolic lines)

2.2. Patch Fitting

Bookstein [Book79] has presented one of the earliest significant works on fitting analytic entities to digitised data, in which he was concerned with the fitting of conic sections to scattered data. Subsequent work resulted in the development of a number of algorithms for conic fitting, best summarised in the work of Fitzgibbon and Fisher ([FiFi95] - "A Buyer's Guide to Conic Fitting"). Kumar et al. [KHGB95] as well as Cohen and Cohen [CoCo96] go further by fitting hyperquadric closed surfaces using an energy minimising approach. Fisher and Fitzgibbon [FiFE97] present a method of deriving surface patches from range descriptions, although the approach is limited to human-made CAD objects with a restricted range of types of patches. Lukacs et al. [LuMM98] also present a least squares fitting approach for similar types of data, although this is based on attempting to fit a number of types of patch (plane, sphere, cone) and select the one with the best fit to classify each part of the surface. Fitzgibbon [FiPF99] addresses the stability problems of generic conic fitting approaches and presents an ellipse-specific fitting algorithm.

2.3. Curvature Estimation

Curvature estimation for 3D surfaces representing natural objects such as faces and human bodies seems to be of particular interest. In particular, a lot of work has been done for faces, primarily because the human face is a relatively simple object with the topology of a deformed cylinder. It is therefore relatively easy to represent the data in cylindrical co-ordinates and treat it as a 2½D problem with one dimension singled out. An early example of that approach is presented by Gordon [Gord91] for 3D faces and a more recent one by Dekker [Dekk00] for human torsos. However, it is impossible to follow such approaches when dealing with a whole human body. The nature and topology of such an object, with its branchings, joints and degrees of freedom, makes it impossible to parameterise it sufficiently as a deformed cylinder (see previous attempts [DoDB99] and [BuDD00]), this is why a full 3D approach (such as the one presented here) is desirable. Sander [SaZu92] uses a Monge form representation to study singularities in curvature direction fields. An attempt at a 3D approach using implicit surfaces can be found in [Hart95], in which a method for calculating fundamental forms and curvatures of implicit surfaces is presented. Hilton and Illingworth [HiIW95] summarise a number of methods for estimating surface curvature estimates and study their reliability statistics. Trucco and Fisher [TrFi95] also use a method of robust curvature estimations (on Monge-type surface representation) for curvature based segmentation of noise data. More recent works include those of Tang and Medioni ([TaMe99] - robust curvature estimation from noisy data using a Tensor Voting scheme) and Mokhtarian et. al ([YuKM99] - fitting of a Monge Patch aligned to the surface geodesics of a smoothed 3D mesh). Har'el [HareXX] follows a novel approach where he approximates the surface locally by means of parabolic curves. Finally, it is worth mentioning the recent curvature calculation works by Csakany and Wallace ([CsWa00] - for triangulated data where the mesh is irregular) as well as Porteous' study of differential features such as ridges and flexcords and their behaviour under smooth transformations [PoPu00]. Finally, there is a significant amount of work on curvature estimation from 3D voxel data, which is not discussed here in detail, as this work is not concerned with voxel data.

2.4. Matching and Registration

Besl has devised a 3D surface registration algorithm currently known as the Iterative Closest Point ICP algorithm [Besl92]. This has become one of the most popular 3D matching algorithms. One of its most attractive features is that it works for almost any type of surface representation. However, it is optimised to perform best with surfaces where the overlap is partial but the shape is very similar in the overlapping area. As mentioned in [BiFi96], ICP is likely to converge to a local minimum that does not correspond to the correct registration between model and data. Moreover, it cannot cope with situations in which the data points are not a subset of the model points or vice-versa. The latter two are frequently the case when dealing with 3D human body surface data from different sources, and this has been one of the major motivations for the work presented in this paper. Bispo and Fisher [BiFi96] build their free-form surface matching algorithm using a modified version of ICP that uses *a priori* knowledge of the correct registration. An example of registration based purely on differential properties is the work of Feldmar and Ayache [FeAy94]. Recent examples of matching applications with human data are the ones by Ruiz and Buxton ([RuBu01] - fitting surfaces to scans of clothed people) and by Hutton ([Hutt01] - on human faces using a dense mesh parameterisation). Finally, it is worth mentioning the work on matching using deformable models such as Snakes (McInerney and Terzopoulos [McTe97]), Active Shape Models (Cootes, Taylor et al. [CTCG95]) and the remarkable application to human bodies (Hilton [Hilt99] – realistic avatars), all of which may utilise differential information for improved performance.

3. Methodology

The idea behind the proposed algorithm is quite simple. To assess the curvature at each point in the given point cloud, the surface is *locally* approximated by an analytic representation ('surface patch'). The differential properties of the patch at the point of interest are then calculated analytically and assigned back to the point. The process is repeated for each point in the point cloud. The analytic representation of choice is an implicit surface of the form $F(x,y,z) = 0$. The reason for choosing this representation is that the fitting of such a surface is easy to formulate as a least squares minimisation that can be solved as an eigenproblem. This makes the implementation straightforward and also generates additional information that can be used for a rigorous assessment of the method's reliability and stability. Moreover, this type of representation allows the method to work on any type of point cloud, regardless of the orientation of the underlying surface. It is therefore possible to use it on point clouds made up of registered subsets of points from a group of sensors. This is an advantage that representations of the form $z = f(x,y)$ do not have, since they cannot represent surfaces where a line of the form $(x=x_c, y = y_c)$ intersects the surface at more than one point (e.g. spheres, ellipsoids, and most other conic sections.

For the proposed algorithm to work, the following assumptions must be valid:

- The input data set is a *Point Cloud*. It is not necessary for the point cloud to be connected, although the use of connectivity information wherever available would speed up the implementation.
- The given point cloud is *Reasonably Clean*. It has already been pre-processed to remove points that do not correspond to the original surface. A certain level of noise is accepted within the surface points, as long as it is an order of magnitude smaller than the size of the object represented (as the first step is a least-squares fitting procedure it is important in the current implementation that there are no outliers in the data; it may be possible, however, in subsequent implementations to reject outliers or to use a robust statistic).
- The surface must be *Sufficiently Sampled*. The point cloud must be sufficiently dense so that a sphere centred on any point on the sampled surface contains only neighbours of the centre point, at least up to second order, and does not contain any points that do not belong to the local surface manifold around the point.
- The point cloud represents a *Significant Coverage* of the original surface. This affects only the use of the results. No curvature is calculated at areas of the object surface not covered by the point cloud, so if the results are to be used for a matching application, the set of features detected will only exist for the covered areas.

The steps of the algorithm are as follows: For every point P in the set:

- A neighbourhood of points (size N) around P is selected. At this stage, connectivity information, if available, may be utilised in order to reduce the search space and improve computational efficiency.
- A quadric patch $F(x,y,z) = 0$ is fitted onto the neighbourhood of points.
- A projection P_0 of P onto the patch is calculated, such that $F(P_0) = 0$.
- The curvature properties of F are calculated at P_0 and assigned back to P.

The steps of the algorithm are discussed in detail in the sections that follow.

3.1. Initial Data Set

We assume that a scanner delivers a set of coordinates $(x(i),y(i),z(i))$ for $i=1,...,N$, say, in a cloud of data points sampled from the body surface. Our aim is to find the form of the surface within some small neighbourhood $N(s)$ of a point s on the surface and hence, for example, to estimate the curvature there. To do so, we choose a local analytic approximation to the surface and fit it to the data points in $N(s)$. It is important that the representation of the analytic approximation used does not single out any coordinate axis. There are thus two choices (see, for example, [Krey59]), namely: (i) a function $F(x,y,z) = 0$, or (ii) a parametric representation: $x = x(u,v)$, $y = y(u,v)$, $z = z(u,v)$. Although the parametric form (ii) is usually preferred in differential geometry, here it presents the additional problem of finding the surface parameters $(u(i), v(i))$ of each point i in $N(s)$. There is no such problem with the function F in (i) and, indeed, this type of representation seems to have been used quite often in fitting to range data from man-made objects. To see what happens, we shall use a quadric form:

$$ax^2 + by^2 + cz^2 + 2exy + 2fyz + 2gzx + 2lx + 2my + 2nz + d = 0$$

which can conveniently be represented by using homogeneous co-ordinates:

$$\begin{bmatrix} x & y & z & 1 \end{bmatrix} \begin{bmatrix} a & e & g & l \\ e & b & f & m \\ g & f & c & n \\ l & m & n & d \end{bmatrix} \begin{bmatrix} x \\ y \\ z \\ 1 \end{bmatrix} = 0$$

or, in matrix vector form: $x^T Ux = 0$ where U is a real symmetric matrix. For simplicity, let's choose the point $(x(s), y(s), z(s))$ as the local origin. This can be done, although it is not obvious that it is best to do so. For example, the fitting may be mathematically more stable if we choose the centroid of the points in $N(s)$ to be the origin (see [HaZi00]).

3.2. Local Patch Fitting

If there are enough points in the neighbourhood $N(s)$, then each datum (x, y, z) will n?t lie perfectly on the surface F, i.e. we shall have:

$$ax^2 + by^2 + cz^2 + 2exy + 2fyz + 2gzx + 2lx + 2my + 2nz + d = e$$

Although this is not a measure of *Euclidean* distance from the surface, (it is, in fact, known as the *algebraic* distance) if we have enough data points (x,y,z) in N (i.e. 9 or more, as we shall see) then we want in the usual way:

$$\min\left\{\sum_{x,y,z\in N}\varepsilon^2\right\} \Rightarrow \min\left\{\sum_{x,y,z\in N}F^2(x,y,z)\right\}$$

Since the quadric expression is homogeneous in $(a,...,g)$, the minimum of the above would be given by $a=b=c=...=g=0$. We therefore need to introduce a constraint, such as:

$$a^2 + b^2 + c^2 + d^2 + 2e^2 + 2f^2 + 2g^2 + 2l^2 + 2m^2 + 2n^2 = 1 \qquad \text{(i.e. } tr(U^T U) = 1\text{)}$$

This is algebraically convenient, but we might wish instead that the normal to the surface at $x = y = z = 0$ is of unit length. Since the normal is defined by:

$$\underline{\nabla}F = 2\begin{bmatrix} ax+ey+gz+l \\ by+ex+fz+m \\ cz+fy+gx+n \end{bmatrix} \Rightarrow \left.\underline{\nabla}F\right|_{x=y=z=0} = 2\begin{bmatrix} l \\ m \\ n \end{bmatrix} \Rightarrow \text{we would want } l^2 + m^2 + n^2 = ¼$$

and that l, m, n are proportional to the direction cosines of the surface normal at the origin, i.e. at the point S of interest. If we can guarantee that l, m, n are never all zero, a choice like $l^2 + m^2 + n^2 = ¼$ might be geometrically convenient. Note that when $l = m = n = 0$, the surface has no normal at the origin and must therefore be degenerate there, i.e. we have two sheets intersecting along a line through 0 (a degenerate hyperboloid) or at the point 0 (a kind of a cone).

3.3. Minimisation

Our minimisation problem is expressed as: $\min\left\{\sum_{x,y,z\in N}F^2(x,y,z)\right\}$

subject to the constraint $a^2 + b^2 + c^2 + d^2 + 2e^2 + 2f^2 + 2g^2 + 2l^2 + 2m^2 + 2n^2 = 1$. The details of the solution are provided in Appendix I. The problem eventually reduces to a 10x10 real symmetric eigenproblem of the form $A = D^T D$ where D is the Nx10 'design matrix', each row of which is built up by the following elements:

$$\begin{bmatrix} x_i^2 & y_i^2 & z_i^2 & x_i y_i & y_i z_i & x_i z_i & x_i & y_i & z_i & 1 \end{bmatrix}, \text{ where } i = 1,...,N$$

This matrix has 10 real eigenvalues and 10 corresponding eigenvectors. The coefficients of the eigenvector corresponding to the *smallest* eigenvalue $?_1$ are the coefficients $a, b, c, e, f, g, l, m, n, d,$ of the quadric surface that best approximates the point cloud locally around P. In fact, the value of $?_1$ itself is the value of the squared error function that was being minimised, so this value can be used to assess the quality of fit. Additionally, by sorting the eigenvectors of A according to the magnitude of the corresponding eigenvalue (in ascending order), we also acquire the nine next best fits to the point cloud. Figure 1 illustrates some results of the quadric patch fitting on test data representing surfaces of known type.

3.4. Closest Point Selection

As a result of the nature of least-squares fitting, there is no constraint to guarantee that $F(P) = 0$ i.e. that the point of interest lies exactly on the quadric patch fitted around its neighbourhood. In general, however, it is safe to assume that $F(P)$ is very close to zero (generally proportional to the square root of $?_1$). It is therefore sufficient to find a point P_0 on F that is as close as possible to P. It would be ideal to locate the point on F that is *exactly the closest* to P. However, it is not convenient to do this in practice, as it would require calculation of the normal n_0 to F, that passes through P and

then calculation of P_0 as the intersection between n_0 and F. Unfortunately, the resulting formulation of the problem is a 6^{th}-degree equation with no closed-form solution. An iterative approach would be computationally expensive, so we chose instead to calculate a direction n_0 that approximates the surface normal. In the current implementation we do so as follows (Figure 2):

We select three lines n_1, n_2 and n_3 that pass through P. For best results we choose them to be orthogonal to each other, and in order to simplify the implementation we can choose them parallel to the axes of the orthogonal coordinate system used. For each of them we calculate the intersections P_i with F. This problem reduces to a second degree equation that is easy to solve and has either zero, one, or two solutions. In the case of zero solutions, we reject n_i from our set of options. In the case of two solutions, we select the one that corresponds to the smaller distance d_i between P and P_i. In addition, we set a new line n_4 to be the mean of the remaining lines and calculate its intersection P_4 and its distance d_4 from F. We now have up to four points P_i that are likely approximations to the ideal point P_0. We select the one (P_{min}) that corresponds to the smallest $d_i = d_{min}$, and set $P_0 = P_{min}$.

The benefit of this approach is that it does not require an indefinite number of iterations, while at the same time it allows a level of refinement of our estimate. We therefore end up with a point P_0 that is a sufficiently accurate approximation to the point on F closest to P that the curvature properties of the surface are not significantly altered.

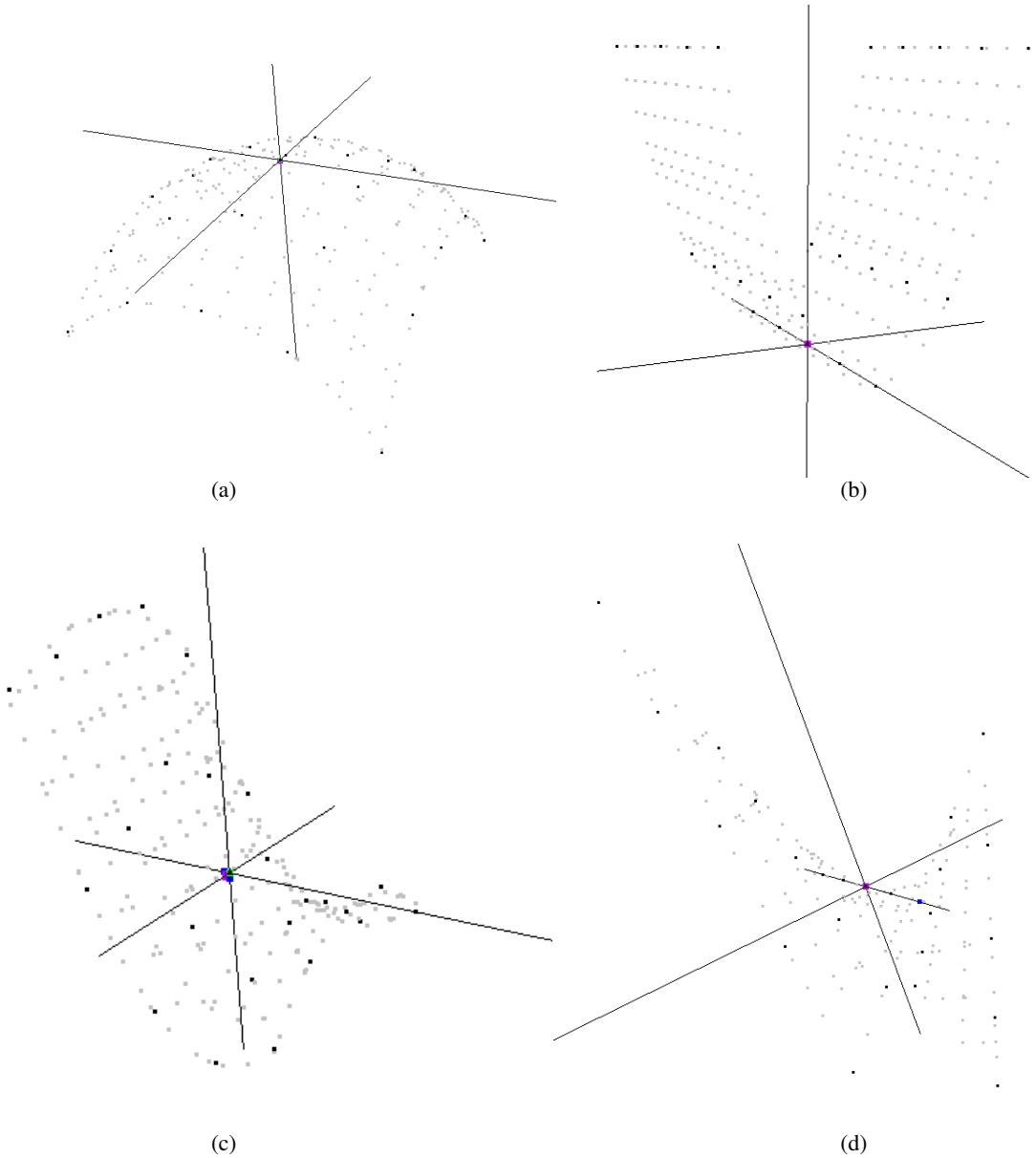

Figure 1: *Results of the quadric patch fitting for test data representing surfaces of known types: (a) elliptic, (b) parabolic, (c) soft saddle, (d) steep saddle. Black dots represent the test data points, grey dots are sample points on the fitted quadric. The lines shown are the axes of the coordinate system, also used as the lines for calculation of the closest points (intersections marked with a blue dot where appropriate).*

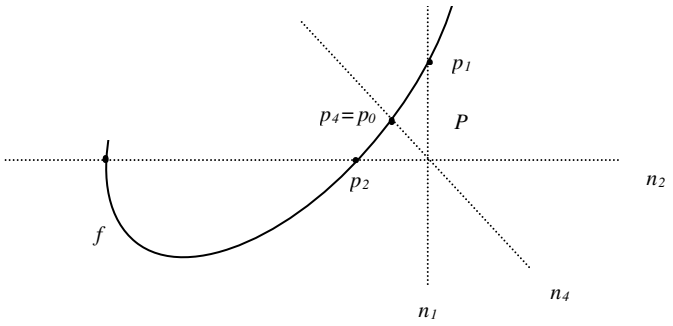

Figure 2: *Illustration of the closest point calculation. In the case illustrated, p_4 is the one closest to p so it is selected as the best estimate.*

3.5. Curvature Calculation

As stated, our objective is to retrieve the surface's analytical geometry from *F*. However, we need to be careful as the implicit form *F(x,y,z) = 0* is not the usual parametric form encountered in most of the differential geometry literature. Moreover, we cannot easily convert the homogeneous implicit form to a parametric form, as this will disturb the numerical stability of the method. In order to calculate the curvature from the patch, there are thus two approaches as discussed below.

3.5.1. Quadratic Forms

As described in chapter 10 of [BeGo88], if *F(x,y,z) = 0* is an implicit surface in R^3, then the Gaussian and mean curvature may be calculated as follows.

Gaussian (total) curvature: Define *a*, *b*, *c* by the identity: $$\left|M\right| = \begin{vmatrix} F'' - \lambda I & F' \\ {}^{t}F' & 0 \end{vmatrix} = a + b\lambda + c\lambda^2$$

where *F'* is the vector of first order partial derivatives of *F* and *F''* is the matrix of second partial derivatives and *I* is the identity matrix. In this notation we have:

$$K = \frac{a/c}{F_x^2 + F_y^2 + F_z^2}, \qquad \text{and}$$

Mean curvature: Using the same notation:

$$H = -\frac{b/c}{2\sqrt{F_x^2 + F_y^2 + F_z^2}}$$

The table below shows the values of Gaussian and mean curvatures that were returned for the test patches pictured in figure 1:

Curvature	*(a) – elliptic*	*(b) - parabolic*	*(c) – soft saddle*	*(d) steep saddle*
Gaussian (K)	0.12	0.00	-0.12	-0.12
Mean (|H|)	0.39	0.99	2.44	4.32

It is easy to verify that the figures are valid and correspond to the definition of surface geometry according to curvature values.

If we want to determine the principal directions, we can take the bisectors of the asymptotic directions, which are the vectors *v* simultaneously satisfying *F'(v) = F''(v,v) = 0*, where: *F'* and *F''* are the first and second derivative forms of *F* [Spi79, vol V, p204-205]. However, this is problematic for elliptic points, where there are no asymptotic directions but we still need exactly two curvature directions. We are therefore developing an alternative approach in which the directions of principal curvature may be calculated directly from matrix M.

3.5.2. Fundamental Forms

Alternatively, we can calculate the curvatures of *F* at *P* as follows: We calculate (see Appendix II) the coefficients *E*, *F*, *G* of the first fundamental form and the coefficients *L*, *M*, *N* of the second fundamental forms. Then, by setting:

$$A = \begin{bmatrix} L & M \\ M & N \end{bmatrix} \text{ and } B = \begin{bmatrix} E & F \\ F & G \end{bmatrix}$$

the eigenvalues $k1, k2$ of $B^{-1}A$ are the values of the principal curvatures. The values of the Gaussian curvature (K) and the mean curvature (H) are therefore given by:

$$K = k_1 \cdot k_2 \qquad \text{and} \qquad H = \frac{1}{2}(k_1 + k_2)$$

This approach seems to generate more stable results in practice than those obtained from the method described in 3.5.1, although in theory both approaches should be equally stable. However, this approach does not seem to generate sufficient information for easy calculation of the principal curvature directions. If the surface were in Monge form, it would be sufficient to calculate the eigenvectors of $B^{-1}A$, and these would be the principal directions. They are 2D vectors, but this is sufficient in Monge form since there is a set orientation of the 3D surface around its normal, which can be used to relate the 2D vectors to the three dimensional space.

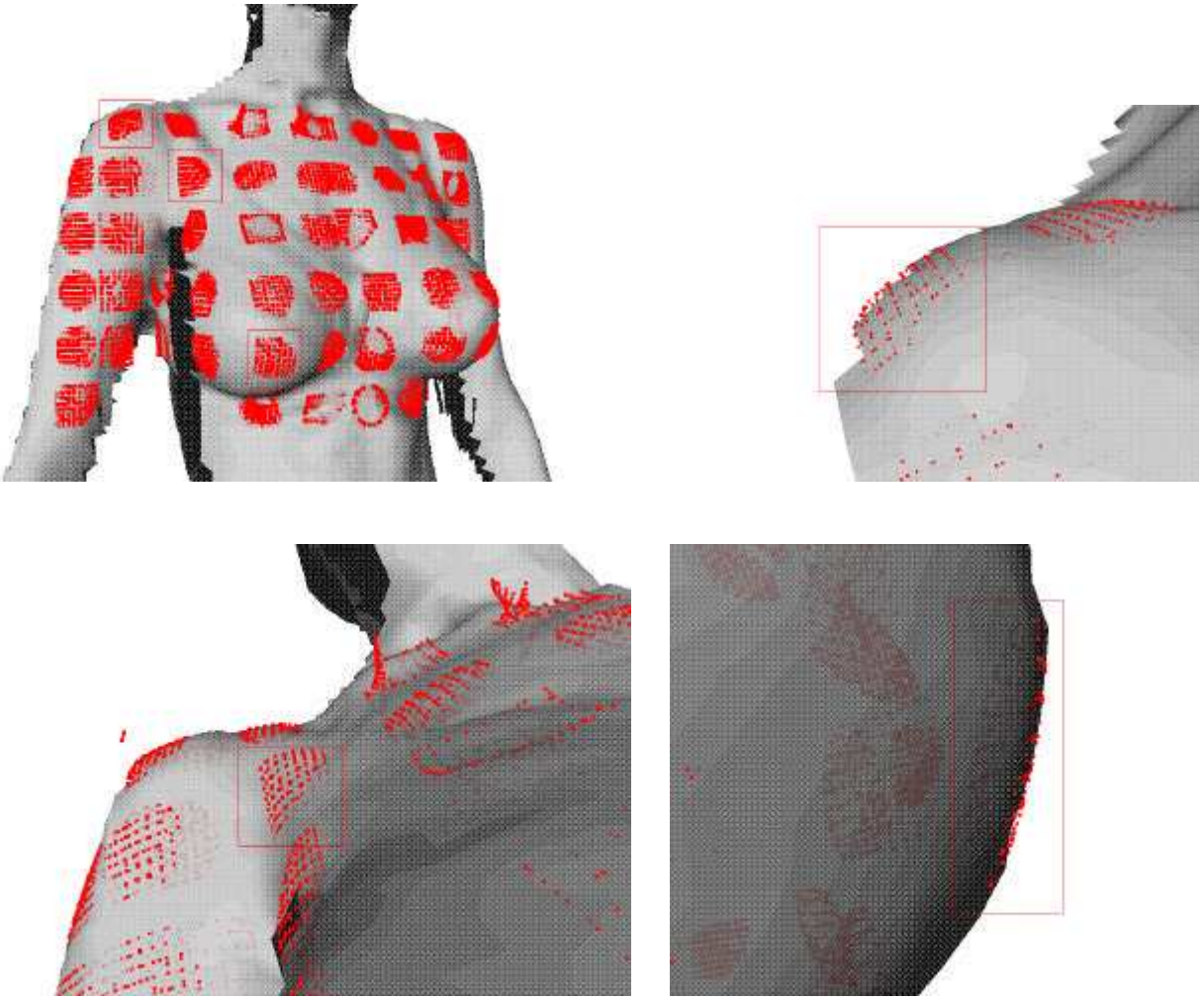

Figure 3: *Application of the proposed patch fitting algorithm to real 3D scanner data. Top left: upper torso with selected fitted patches. The three patches marked are (from top left to bottom right): parabolic, saddle and elliptic. Top right, bottom left and bottom right: close-up views of the marked patches in the same order.*

4. Results

Figure 3 shows the application of the proposed quadric patch fitting algorithm on real data acquired using 3D scanning hardware. The cases illustrated are the three usual ones: elliptic, parabolic, and saddle. It can easily be seen that in all cases there is a satisfactory approximation of the surface around the point of interest.

In addition, Figures 4 and 5 show the results of mapping the mean and Gaussian curvature results onto the bodies of two sample subjects, one male and one female respectively[1]. Once again, the mapping indicates that the curvature results are satisfactory, with flat, elliptic and saddle regions shown as expected.

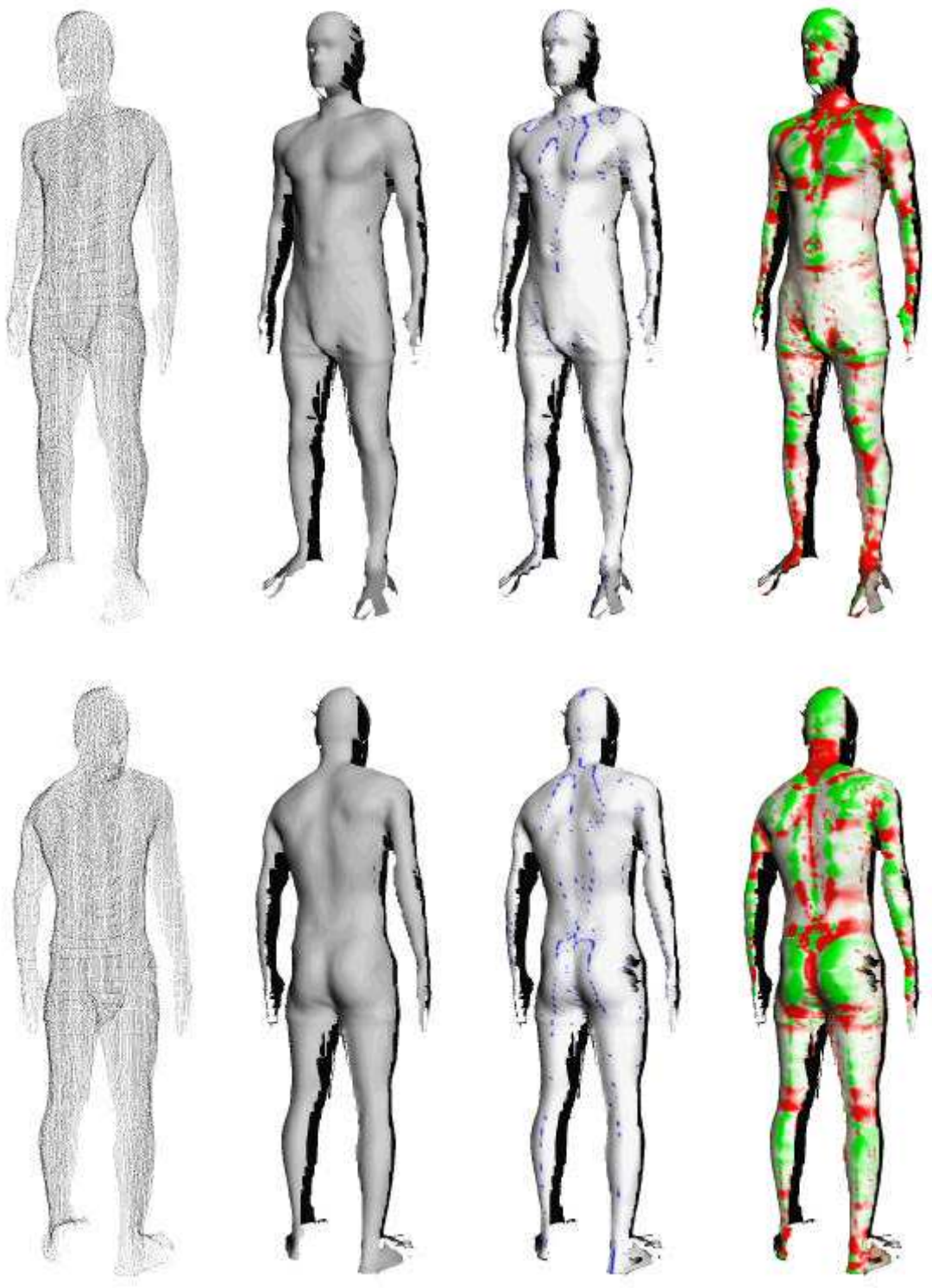

(a) (b) (c) (d)

Figure 4: *Curvature maps on a whole body scan of a male subject. Top row: front view. Bottom row: rear view. From left to right: (a) point cloud, (b) smooth shaded triangulated surface, using the connectivity information supplied, (c) mean curvature, (d) Gaussian curvature. In case (c), blue areas indicate points of high mean curvature, which are candidate ridges and crests. In case (d), white areas are locally flat; green areas indicate positive Gaussian curvature (extrusions and recesses); red areas indicate negative Gaussian curvature (saddle regions).*

[1] It is essential to view those images in full colour to appreciate the quality of the results. The pictures from this paper are available for viewing in full colour at http://www.cs.ucl.ac.uk/staff/i.douros/pics_curvmap.html

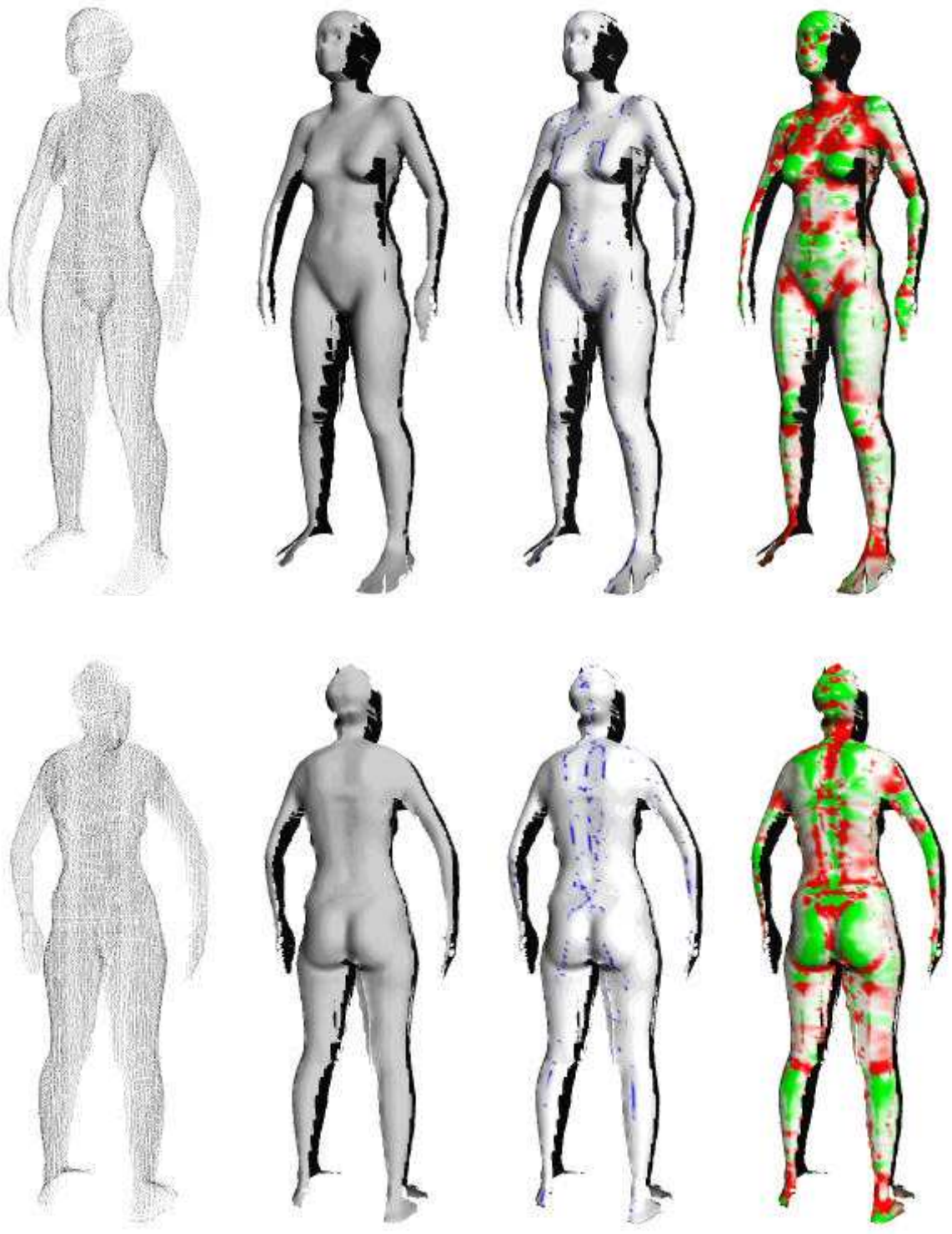

Figure 4: *Curvature maps on a whole body scan of a female subject. Top row: front view. Bottom row: rear view. From left to right: (a) point cloud, (b) smooth shaded triangulated surface, using the connectivity information supplied, (c) mean curvature, (d) Gaussian curvature. In case (c), blue areas indicate points of high mean curvature, which are candidate ridges and crests. In case (d), white areas are locally flat; green areas indicate positive Gaussian curvature (extrusions and recesses); red areas indicate negative Gaussian curvature (saddle regions).*

In the examples illustrated in figures 4 and 5 the scans used were 'raw' scans, not fully processed reconstructed surfaces, hence there are gaps in the surface as usually occur for 'raw' scans. The algorithm works equally well with point clouds representing fully reconstructed surfaces, as all it requires is the points and their neighbours. In addition, the algorithm will work without any connectivity information at all, except in that case the search for a point's neighbours will be of greater computational complexity. It is also likely to be more difficult to render a clear visualisation of the results in such cases, but this should not affect the quality of the numerical results obtained.

Finally, Figure 6 shows a comparison of results for the two approaches for calculating the values of mean and Gaussian curvature, namely the using the quadratic form presented in 3.5.1 and using the fundamental form presented in 3.5.2. Although in neither of the two cases are the results intuitively wrong, it appears that use of the fundamental form is less sensitive to noise in regions around the zero-crossings of Gaussian curvature.

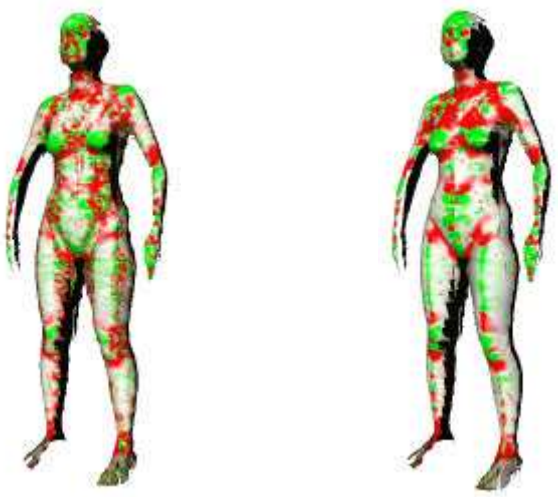

(a) (b)

Figure 6: *Comparison of curvature mapping results using different methods of calculation of mean and Gaussian curvature from the analytic representation of the implicit quadric patch: (a) using the quadratic forms, (b) using the fundamental forms.*

5. Future Work

Research efforts are currently focused on the calculation of principal curvature directions using the results of the proposed algorithm. This will complete the compilation of a rich set of information that will allow the identification of significant features on the surface such as parabolic lines, umbilics, ridges and flexcords. We are planning subsequently to use this information in order to drive a 3D matching algorithm and deform seamless body avatars to match real, whole body datasets. In addition, we are planning a rigorous and extensive study of the stability, reliability and accuracy of the numerical results of the algorithm.

6. Acknowledgements

The authors wish to thank: The DTI-supported ForeSIGHT 3DCentre Project, under the sponsorship of which most of the work has been carried out, Hamamatsu Photonics for supplying the Body Lines Scanner used for the acquisition of 3D data, and Mr. Tim Hutton of the Eastman Dental Institute for providing parts of source code used in the implementation of the proposed algorithm.

APPENDIX I: Least squares Minimisation of Quadric Patches

Our minimisation problem is expressed as:

$$\min\left\{\sum_{x,y,z\in N} F^2(x,y,z)\right\}$$

It is convenient to use matrix notation, i.e:

$$\min_{m_{\alpha,\beta}}\left\{\sum_{x,y,z\in N}\left(\sum_{\alpha\le\beta} x_\alpha u_{\alpha\beta} x_\beta\right)^2\right\}$$

subject to:

$$\sum_{\alpha\le\beta} u_{\alpha\beta}^2 = 1$$

where $a, \beta = 1,...,4$, stand for the four components of the homogeneous vectors Since terms in x_iy_i, y_ix_i, etc are indistinguishable, we restrict a to be less than or equal to β and the elements $u_{a\beta}$ of the matrix are appropriately defined. If we introduce a Lagrange multiplier *?*, we thus have, subject to the aforementioned constraint:

$$\min_{m_{\alpha,\beta}}\left\{\sum_{x,y,z\in N}\left(\sum_{\alpha\le\beta} x_\alpha u_{\alpha\beta} x_\beta\right)^2 + \lambda\left(1-\sum_{\alpha\le\beta} u_{\alpha\beta}^2\right)\right\}$$

On differentiating w.r.t. $u_{?d}$, for $\gamma \le \delta$, we thus find:

$$\sum_{x,y,z\in N} x_\gamma x_\delta \sum_{\alpha\le\beta} x_\alpha u_{\alpha\beta} x_\beta - \lambda u_{\gamma\delta} = 0 \quad \Rightarrow \quad \sum_{\alpha\le\beta}\left(\sum_{x,y,z\in N} x_\gamma x_\delta x_a x_\beta \right) u_{\alpha\beta} = \lambda u_{\gamma\delta}$$

which is of a matrix eigenvalue-eigenvector form $Au = ?u$, where A is the 10x10 matrix for all $a,\beta,?,d$:

$$\sum_{x,y,z\in N} x_\gamma x_\delta x_a x_\beta$$

and m is the 10x1 column vector constructed from the independent elements of the symmetric matrix M. Alternatively, A can be expressed as $A = D^T D$ where D is the Nx10 'design matrix', each row of which may be built up by the following elements:

$$\left[x_i^2 \quad y_i^2 \quad z_i^2 \quad x_i y_i \quad y_i z_i \quad x_i z_i \quad x_i \quad y_i \quad z_i \quad 1\right], \text{ where } i = 1,\ldots,N$$

If, as usual, we normalise the eigenvectors u to unity, the constraint is automatically satisfied and we see that:

$$\sum_{x,y,z\in N} \varepsilon^2 = \sum_{x,y,z\in N} F^2(x,y,z) = \sum_{x,y,z\in N}\left\{\sum_{\alpha\le\beta}\left(x_\alpha u_{\alpha\beta} x_\beta\right)^2\right\} = \sum_{x,y,z\in N}\sum_{\alpha\le\beta} x_\alpha u_{\alpha\beta} x_\beta \sum_{\gamma\le\delta} x_\gamma u_{\gamma\delta} x_\delta$$

$$\Rightarrow \quad \sum_{x,y,z\in N} \varepsilon^2 = \sum_{\alpha\le\beta} u_{\alpha\beta} \sum_{\gamma\le\delta}\left(\sum_{x,y,z\in N} x_\alpha x_\beta x_\gamma x_\delta \right) u_{\gamma\delta} = \sum_{\alpha\le\beta} u_{\alpha\beta} \sum_{\gamma\le\delta} \mathrm{A}_{\alpha\beta\gamma\delta} u_{\gamma\delta} = \sum_{\alpha\le\beta} \lambda u_{\alpha\beta} u_{\alpha\beta}$$

$$\text{i.e: } \sum_{x,y,z\in N} \varepsilon^2 = \lambda$$

Thus the best fit surface is obtained from the components of the lowest eigenvector of the matrix A defined above. Thus, we follow an approach similar to the one presented in [FIPF99], and build a 10x10 eigenproblem where there is exactly one unknown for each quadric coefficient.

APPENDIX II: Fundamental forms of implicit surfaces.

Based on the calculation of fundamental forms as presented by Hartmann [Hart95], let:

$F(x,y,z) = ax^2+by^2+cz^2+exy+fyz+gxz+lx+my+nz+d = 0$ an implicit quadric surface in R^3.

The first order partial derivatives of F are:

$$F_x = 2ax+ey+gz+l$$
$$F_y = 2by+ex+fz+m$$
$$F_z = 2cz+fy+gx+m$$

Then the coefficients E, F, G of the *First Fundamental Form* are:

$$E = 1+\frac{F_x^2}{F_z^2}, \qquad F = \frac{F_x F_y}{F_z^2}, \qquad \text{and } G = 1+\frac{F_y^2}{F_z^2} \qquad \text{hence: } EG - F^2 = \frac{F_x^2+F_y^2+F_z^2}{F_z^2}$$

Furthermore, the second order partial derivatives are:

$$F_{xx} = 2a \qquad F_{xy} = F_{yx} = e$$
$$F_{yy} = 2a \qquad F_{yz} = F_{zy} = f$$
$$F_{zz} = 2a \qquad F_{xz} = F_{zx} = g$$

And the magnitude of the gradient is: $\left|\nabla F\right| = \sqrt{F_x^2+F_y^2+F_z^2}$

Then, the coefficients L, M, N of the *Second Fundamental Form* are:

$$L = \frac{1}{F_z^2\left|\nabla F\right|}\begin{vmatrix} F_{xx} & F_{xz} & F_x \\ F_{zx} & F_{zz} & F_z \\ F_x & F_z & 0 \end{vmatrix}, \; M = \frac{1}{F_z^2\left|\nabla F\right|}\begin{vmatrix} F_{xy} & F_{yz} & F_y \\ F_{zx} & F_{zz} & F_z \\ F_x & F_z & 0 \end{vmatrix}, \; N = \frac{1}{F_z^2\left|\nabla F\right|}\begin{vmatrix} F_{yy} & F_{yz} & F_y \\ F_{zy} & F_{zz} & F_z \\ F_y & F_z & 0 \end{vmatrix}$$

References

[BeGo88] Berger, M., Gostiaux, B., 'Graduate Texts in Mathematics – Differential Geometry: Manifolds, Curves and Surfaces', Springer Verlag 1988, ISBN 0-387-96626-9.

[Besl92] Besl, P.J., 'A method for registration of 3D shapes', IEEE Trans. PAMI, Vol.14, No.2, February 1992, pp239-256.

[BiFi96] Bispo E.M, Fisher R.B, "Free-form Surface Matching for Surface Inspection", Procs of 6th IMA Conf. on Mathematics of Surfaces, 1996.

[Book79] Bookstein, F.L., 'Fitting Conic Sections to Scattered Data', Computer Graphics and Image Processing, Part 9, 1979, pp56-71.

[BrGT96] Bruce, J.W., Giblin, P.J., Tari, F., ''Ridges, Crests and Sub-Parabolic Lines of Evolving Surfaces', IJCV 18(3), pp195-210, 1995-1996.

[BuDD00] Buxton B., Dekker L., Douros I., Vassilev T., "Reconstruction and Interpretation of 3D Whole Body Surface Images", Scanning 2000 Proceedings, Paris, May 2000.

[CoCo96] Cohen I, Cohen L, "A Hybrid Hyperquadric Model for 2-D and 3-D Data Fitting", Computer Vision and Image Understanding, Vol 63, No 3, pp527-541, May 1996.

[CsWa00] Csakany, P., Wallace, A.M., 'Computation of Local Differential Parameters on Irregular Meshes', The Mathematics of Surfaces IX, Institute of Mathematics and its Applications, Cambridge 2000, pp19-33.

[CTCG95] Cootes, T.F., Taylor, C.J., Cooper, D.H., Graham, J., 'Active Shape Models - Their Training and Application', Computer Vision and Image Understanding, January 1995.

[Dekk00] Dekker,L., '3D Human Body Modelling from Range Data', PhD Thesis, University College London, 2000.

[DoDB99] Douros I., Dekker L., Buxton B., "An Improved Algorithm for Reconstruction of the Surface of the Human Body from 3D Scanner Data Using Local B-spline Patches", mPeople Workshop Proceedings, IEEE-ICCV99, pp29-36, Corfu, Greece, September 1999.

[Gord91] Gordon. A. P., "Face recognition based on depth maps and surface curvature", Procs of SPIE Conference on Geometric Methods in Computer Vision, San Diego CA, 1991.

[FeAy94] Feldmar J, Ayache N, "Rigid and Affine Registration of Smooth Surfaces Using Differential Properties", Lecture Notes in Computer Science, Vol 801, ECCV 1994, pp397-406.

[FiFE97] Fisher R.B, Fitzgibbon A.W, Eggert D.W, "Extracting Surface Patches from Complete Range Descriptions", IEEE Vol 1, 1997, pp148-155.

[FiFi95] Fitzgibbon A.W, Fisher R.B, 'A Buyer's Guide to Conic Fitting', Proc. BMVC 1995, Vol 2, pp513-522.

[FiPF99] Fitzgibbon, A., Pilu, M., Fisher, R.B., 'Direct Least Square Fitting of Ellipses', IEEE Trans. PAMI, Vol.21, No.5, May 1999, pp476-480.

[HareXX] Har'el, S., "Curvatures of curves and surfaces – a parabolic approach", Department of Mathematics, Technion – Israel Institute of Technology.

[Hart95] Hartmann E., 'Blending and Implicit with a Parametric Surface', Computer Aided Geometric Design 12 (1995), 825-835, esp. appendix on implicit surfaces (p.834).

[HaZi00] Hartley, R., Zisserman, A., 'Multiple View Geometry', Cambridge University Press, March 2000

[HiIW95] Hilton A, Illingworth J, Windeatt T, "Statistics of Surface Curvature Estimates", Pattern Recognition, Vol 28, No 8, pp1201-1221, 1995

[Hilt99] Hilton, A., 'Towards Model-Based Capture of a Persons Shape, Appearance and Motion', mPeople Workshop Proceedings, IEEE-ICCV99, pp37-44, Corfu, Greece, September 1999.

[Hutt01] Hutton T, Buxton B F, Hammond P, 'Dense Surface Point Distribution Models of the Human Face', Proc. IEEE Workshop on Mathematical, Methods in Biomedical Image Analysis, December, Kauai, Hawaii. pp. 153-160.

[KHGB95] Kumar S, Han S, Goldgof D, Bowyer K, "On Recovering Hyperquadrics from Range Data", IEEE Trans on Pattern Analysis and Machine Intelligence, Vol 17, No 11, 1995, pp1079-1083.

[Krey59] Kreyszig,E., 'Differential Geometry', Mathematical Expositions No. 11, Oxford University Press 1959.

[LuMM98] Lukacs G, Martin R, Marshall D, "Faithful Least-Squares Fitting of Spheres, Cylinders, Cones and Tori for Reliable Segmentation", Lecture Notes in Computer Science, Vol I, ECCV 1998, pp671-686.

[McTe97] McInerney, T., Terzopoulos, D., 'Medical Image Segmentation Using Topologically Adaptable Surfaces', Proc. CVRMed'97, Grenoble, France, March 1997.

[PoPu00] Porteous, I.R., Puddephat, M.J., 'Landmarks of a Surface', The Mathematics of Surfaces IX, Institute of Mathematics and its Applications, Cambridge 2000, pp114-125.

[Port94] Porteous, I., "Geometric Differentiation" , Chapters 1,6,10-16, Cambridge University Press 1994.

[RuBu01] Ruiz, M.C., Buxton, B., "A Model-Based Procedure for Fitting a Surface to Scans of Clothed People", Scanning 2001 Proceedings, Paris, May 2001.

[SaZu92] Sander, P.T., Zucker, S.W., "Singularities of principal direction fields from 3d images", IEEE Trans PAMI Vol 14, No 3, March 1992.

[TaMe99] Tang,C.K., Medioni,G., 'Robust Estimation of Curvature Information from Noisy 3D Data for Shape Description', IEEE 1999

[TrFi95] Trucco E, Fisher R.B, "Experiments in Curvature-Based Segmentation of Range Data", IEEE Trans. on Pattern Analysis and Machine Intelligence, Vol 17, Part 2, 1995, pp171-182.

[YuKM99] Yuen, P., N. Khalili, and F. Mokhtarian, "Curvature Estimation on Smoothed 3-D Meshes", Proc. British Machine Vision Conference, pp. 133-142, Nottingham, 1999.